Available online at www.sciencedirect.com
SCIENCE DIRECT
Biochimica et Biophysica Acta 1716 (2005) 11 – 18
BIOCHIMICA ET BIOPHYSICA ACTA
BBA
http://www.elsevier.com/locate/bba

Membrane-disruptive abilities of β-hairpin antimicrobial peptides correlate with conformation and activity: A ^{31}P and ^{1}H NMR study

Rajeswari Mani [a], Alan J. Waring [b], Robert I. Lehrer [b], Mei Hong [a,*]

[a] *Department of Chemistry, Iowa State University, Ames, IA 50011, USA*
[b] *Department of Medicine, University of California at Los Angeles School of Medicine, Los Angeles, CA 90095, USA*

Received 18 February 2005; received in revised form 8 August 2005; accepted 23 August 2005
Available online 7 September 2005

Abstract

The membrane interaction and solution conformation of two mutants of the β-hairpin antimicrobial peptide, protegrin-1 (PG-1), are investigated to understand the structural determinants of antimicrobial potency. One mutant, [$A_{6,8,13,15}$] PG-1, does not have the two disulfide bonds in wild-type PG-1, while the other, [$\Delta_{4,18}$ G_{10}] PG-1, has only half the number of cationic residues. ^{31}P solid-state NMR lineshapes of uniaxially aligned membranes indicate that the membrane disorder induced by the three peptides decreases in the order of PG-1>[$\Delta_{4,18}$ G_{10}] PG-1 ≫[$A_{6,8,13,15}$] PG-1. Solution NMR studies of the two mutant peptides indicate that [$\Delta_{4,18}$ G_{10}] PG-1 preserves the β-hairpin fold of the wild-type peptide while [$A_{6,8,13,15}$] PG-1 adopts a random coil conformation. These NMR results correlate well with the known activities of these peptides. Thus, for this class of peptides, the presence of a β-hairpin fold is more essential than the number of cationic charges for antimicrobial activity. This study indicates that ^{31}P NMR lineshapes of uniaxially aligned membranes are well correlated with antimicrobial activity, and can be used as a diagnostic tool to understand the peptide–lipid interactions of these antimicrobial peptides.
© 2005 Elsevier B.V. All rights reserved.

Keywords: Antimicrobial peptide; PG-1; ^{31}P solid-state NMR; Conformation; Membrane disorder; Solution NMR

1. Introduction

The peptide–lipid interactions of an increasing number of antimicrobial peptides have recently been examined using ^{31}P NMR (for review, see [1,2]). The ^{31}P spectra provide rich information on the response of lipid bilayers to peptide binding, which in turn shed light on the mechanism of action of these peptides. ^{31}P chemical shift anisotropy (CSA) is sensitive to both the lipid phase and the headgroup conformation [3]. The 100% natural abundance and the high gyromagnetic ratio of the ^{31}P spin further make ^{31}P NMR a high-sensitivity probe of peptide–lipid interactions. While wide-line ^{31}P CSA spectra of unoriented proteoliposomes were commonly measured and analyzed, the signals of non-lamellar lipids induced by the peptide usually overlap with the powder pattern of the remaining lamellar bilayer. This spectral overlap limits the structural information that can be extracted [4–6]. To resolve multiple lipid morphologies, macroscopically oriented samples can be prepared for which the ^{31}P signal of each distinct lipid phase is narrowed to a single anisotropic frequency. A number of peptides, such as PG-1, RTD-1, LL-37, and MSI-78 [7–11], have recently been investigated using this uniaxial alignment approach.

Despite the increasing knowledge of the peptide-induced changes of membrane morphology and dynamics, it is not clear whether the observed deviations of the ^{31}P spectral lineshape from that of the lamellar L_α phase occur specifically for membrane-lytic peptides, or whether they are generally true even for non-membrane disruptive peptides as long as the peptide concentration is sufficiently high. Another common underlying assumption in using ^{31}P NMR for understanding peptide–lipid interaction is that the amount of the non-lamellar lipid signals correlates with antimicrobial potency. This assumption remains to be verified. If the membrane disorder

Abbreviations: PG-1, protegrin-1; POPC, 1-palmitoyl-2-oleoyl-sn-glycerol-3-phosphatidylcholine; POPG, 1-palmitoyl-2-oleoyl-sn-glycerol-3-phosphatidylglycerol; POPE, 1-palmitoyl-2-oleoyl-sn-glycero-3-phosphatidylethanolamine; DLPC, dilauroylphosphatidylcholine; DMPC, dimyristoylphosphatidylcholine; DPG, diphosphatidylglycerol

* Corresponding author. Tel.: +1 515 294 3521; fax: +1 515 294 0105.
E-mail address: mhong@iastate.edu (M. Hong).

0005-2736/$ - see front matter © 2005 Elsevier B.V. All rights reserved.
doi:10.1016/j.bbamem.2005.08.008

seen in the ^{31}P spectra can indeed be correlated with biological activity, then one may use ^{31}P NMR as a simple molecular diagnostic tool of the antimicrobial activities of these peptides. In addition to establishing a correlation between ^{31}P spectral disorder and antimicrobial activity, it is important to understand whether and how the conformation of a peptide, dictated by its amino acid sequence, affects its membrane disruptive ability.

In this study, we combine ^{31}P solid-state NMR and ^{1}H solution NMR to examine the membrane-disruptive ability and the solution conformation of two PG-1 derivatives, and relate these to the known antimicrobial activities of these peptides. Protegrin-1 (PG-1) is a β-hairpin peptide with potent and broad-spectrum antimicrobial activities [12,13]. It contains six Arg residues distributed at the two ends of the hairpin, and is stabilized by two cross-strand disulfide bonds. Two PG-1 mutants are studied here. [$A_{6,8,13,15}$] PG-1 replaces all four Cys residues with Ala, while [$\Delta_{4,18}$ G_{10}] PG-1 reduces the number of cationic residues from six to three compared to the wild-type peptide (Fig. 1). The activities of these two mutants have been measured before and found to be more than an order of magnitude weaker than wild type PG-1 [14]. We show here that there is indeed a correlation among membrane disorder, the peptide conformation, and the antimicrobial activity. The least structured peptide causes the weakest membrane disruption and is also the one with the lowest antimicrobial activity.

2. Materials and methods

2.1. Materials

All lipids were purchased from Avanti Polar Lipids (Alabaster, AL) and used without further purification. PG-1 (NH_2-RGGRLCYCRRRFCVCVGR-$CONH_2$), [$A_{6,8,13,15}$] PG-1 and [$\Delta_{4,18}$ G_{10}] PG-1 were synthesized using Fmoc solid-phase peptide synthesis protocols as described previously [7]. In [$A_{6,8,13,15}$] PG-1 (NH_2-RGGRLAYARRRFAVAVGR-$CONH_2$), the four Cys residues are replaced by Ala. In [$\Delta_{4,18}$ G_{10}] PG-1 (NH_2-RGGLCYCRGRF-CVCVG-$CONH_2$), two Arg residues at the N- and C-termini are deleted and Arg_{10} at the hairpin tip is replaced by a Gly (Fig. 1).

2.2. Sample preparation

Glass-plate oriented membranes were prepared using a naphthalene-incorporated procedure [15]. The peptide was dissolved in TFE and mixed with a chloroform solution of the desired lipids. The mixture was dried under a stream of N_2 gas and the dried film was redissolved in a 2:1 mixture of chloroform/TFE containing a five-fold excess of naphthalene with respect to the lipids. The solution was deposited on glass plates (Marienfeld Laboratory Glassware) of ~80 μm thickness and 6 × 12 mm^2 size at a concentration of 0.01–0.02 mg/mm^2. The sample was air-dried for 2 h and then vacuum dried for 5 h to remove all the solvents and naphthalene. The dried membranes were hydrated first by direct deposition of ~1 μL of water per plate and then at 95% relative humidity over a saturated solution of Na_2HPO_4 for 2–3 days. All samples were hydrated at room temperature except DMPC, which was hydrated at 30 °C. Subsequently, the glass plates were stacked, wrapped in parafilm and sealed in a polyethylene bag to prevent dehydration. To ensure reproducibility, most membrane sample series as a function of peptide concentration were repeated 2–3 times. The orientational disorder reported below is the average of these multiple runs.

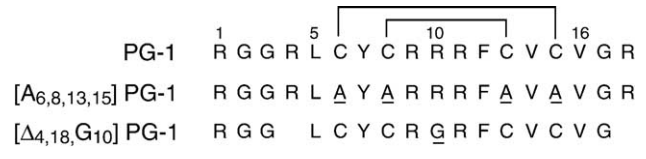

Fig. 1. Amino acid sequence of wild-type PG-1 and its two derivatives, [$A_{6,8,13,15}$] PG-1 and [$\Delta_{4,18}$ G_{10}] PG-1.

Solution NMR samples were prepared by dissolving the peptides in a 5-mM sodium phosphate buffer in 9/1 H_2O/D_2O at pH 6.5. The peptide concentrations were ~3 mM.

2.3. NMR spectroscopy

Static solid-state ^{31}P experiments on oriented peptide–lipid mixtures were carried out on a Bruker DSX-400 spectrometer operating at a resonance frequency of 162.12 MHz for ^{31}P and 400.49 MHz for ^{1}H. A double-resonance probe equipped with a custom-designed rectangular coil with the dimensions of 6 × 12 × 5 mm was used. The samples were inserted into the magnet with the alignment axis parallel to the external magnetic field. The ^{31}P chemical shift was referenced externally to 85% phosphoric acid at 0 ppm. The experiments used a ^{31}P 90° excitation pulse of 5 μs, a ^{1}H decoupling field strength of ~50 kHz, and a recycle delay of 2 s. All ^{31}P spectra were processed with a LB of −10 and a GB of 0.05.

All ^{1}H solution spectra were recorded on a Bruker DRX-500 spectrometer operating at a ^{1}H frequency of 499.867 MHz. TOCSY, NOESY and COSY spectra were acquired using standard protocols [16]. The ^{1}H chemical shift was externally referenced to DSS. Solvent suppression was achieved using the WATERGATE method [17]. Mixing times were 100 ms for TOCSY and 300 ms for NOESY. For the TOCSY experiment, the spin-lock field strength was 6.5 kHz and the DIPSI-2 [18] sequence was used for isotropic mixing.

3. Results

3.1. ^{31}P NMR of uniaxially aligned lipid membranes

We first compare the orientational disorder of anionic lipid bilayers induced by the wild type PG-1 and its two mutants. Previous NMR studies of PG-1 and RTD-1 [8,19] found that these peptides preferentially disrupt anionic membranes while creating reduced disorder in neutral or cholesterol-containing membranes. Thus, anionic lipid bilayers provide a suitable matrix for testing the membrane-disruptive ability of the PG-1 derivatives. We use POPC/POPG bilayers at a 3:1 molar ratio as our first model membrane, as it provides a direct comparison with neutral POPC bilayers and its membrane-surface charge density is analogous to that of bacterial membranes [20]. Fig. 2 shows one representative set of ^{31}P spectra of POPC/POPG bilayers with 0–8 mol% of PG-1, [$\Delta_{4,18}$ G_{10}] PG-1, and [$A_{6,8,13,15}$] PG-1. In the absence of the peptides, the lipid bilayers give rise to a narrow and partially resolved peak at 30.8 ppm, which corresponds to the parallel orientation of the bilayer normal from the magnetic field. The partial resolution in some of the 0% spectra (top row) reflects the slightly different ^{31}P chemical shift anisotropies of POPC and POPG lipids. For the reference PG-1-containing lipids (a), an isotropic peak at 1.5 ppm grew with increasing concentration of PG-1, indicating the formation of micelles or small lipid vesicles upon PG-1 binding [19]. In comparison, the membranes containing [$\Delta_{4,18}$ G_{10}] PG-1 showed mild disorder up to 4% concentration (b). Only when the peptide concentration increased to 8% did a broad peak between −15 ppm and +20 ppm become significant. In contrast, [$A_{6,8,13,15}$] PG-1 causes much less membrane disorder at all concentrations used

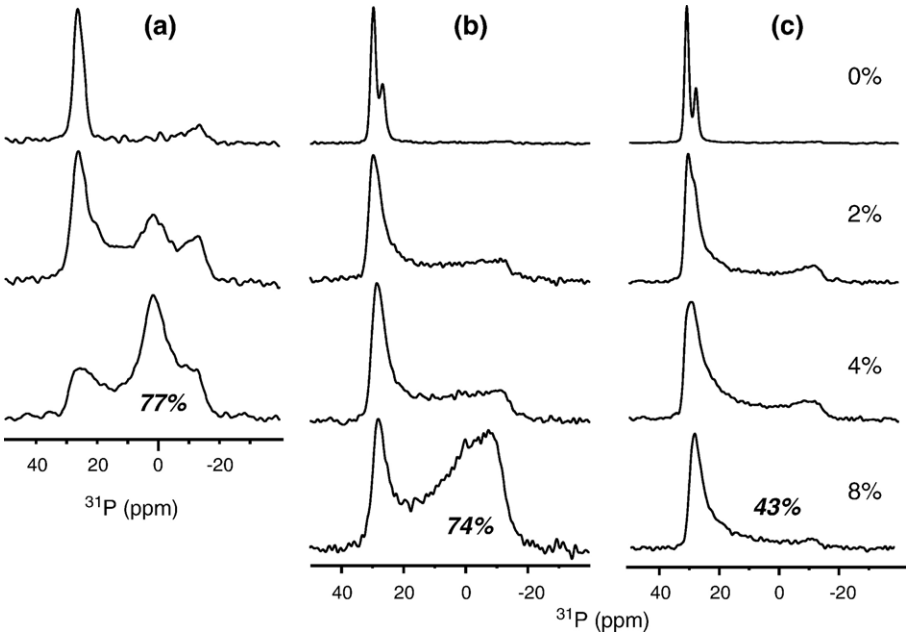

Fig. 2. ^{31}P spectra of oriented POPC/POPG (3:1) bilayers with varying concentrations of (a) PG-1, (b) [$\Delta_{4,18}$ G_{10}] PG-1, and (c) [$A_{6,8,13,15}$] PG-1. The peptide molar concentrations are 0%, 2%, 4% and 8% from top to bottom. The fractional disorder is indicated for the highest concentration in each series. Column (a) is reproduced from Ref. [19].

(c). The main spectral change is the asymmetric broadening of the 0° peak, which reflects an increased mosaic spread of the lipid bilayers [21]. For example, the 0° peak in the 4% [$A_{6,8,13,15}$] PG-1 spectrum corresponds to a mosaic spread of 12°. To compare the membrane disorder more quantitatively, we define fractional disorder as the relative intensity of the spectral region outside the 0°-peak to the total spectral intensity. Averaged over several repeat samples, we found that PG-1 causes 74% fractional disorder at 4% peptide concentration, while [$\Delta_{4,18}$ G_{10}] PG-1 reaches a similar level of disorder (70%) only at 8% peptide concentration, and [$A_{6,8,13,15}$] PG-1 has the lowest fractional disorder, ~45%, even at 8%.

We next examine the effects of the three peptides on POPE/POPG (3:1) bilayers, which mimic the membrane composition of bacteria more closely [20]. Fig. 3 shows oriented ^{31}P spectra of POPE/POPG bilayers in the presence of the peptides. PG-1 shows similar membrane disruptive behavior as towards POPC/POPG bilayers. However, the isotropic peak, at ~3.8 ppm, is no longer well resolved from the rest of the powder intensity (a, bottom). This indicates that the tumbling of the micelles or vesicles caused by PG-1 is slower, which suggests that the POPE/POPG vesicles are larger than the POPC/POPG ones. Similarly, both PG-1 mutants caused reduced membrane disorder (Fig. 3b, c) than towards POPC/POPG bilayers, as indicated by the fractional disorder. There is no significant difference in the membrane disorder between the two mutants towards the POPE/POPG bilayers.

The possibility that the disorder seen in the POPE/POPG spectrum containing 4% PG-1 (Fig. 3a) may result from hexagonal phase lipids can be reasonably ruled out, since the hexagonal phase has an anisotropy half that of the lamellar bilayer phase, and thus would have a 90° frequency of 8.5 ppm and a 0° frequency of −11 ppm. No distinct peaks are observed at these frequencies in the spectra.

To determine how the two PG-1 derivatives interact with more physiological membranes, we measured the ^{31}P spectra of oriented *E. coli* lipid extract, which consists of 57.5% PE, 15.1% PG, 9.8% cardiolipin (or DPG) and 17.6% other lipids by weight (Avanti Polar Lipids). The ^{31}P lineshapes of the two mutants (Fig. 4b, c) confirm their different membrane rupturing

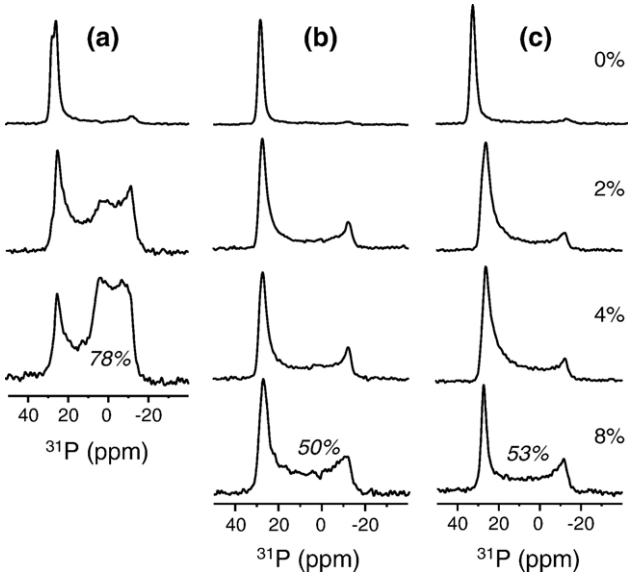

Fig. 3. ^{31}P spectra of oriented POPE/POPG (3:1) membranes in the presence of (a) PG-1, (b) [$\Delta_{4,18}$ G_{10}] PG-1, and (c) [$A_{6,8,13,15}$] PG-1. The peptide concentrations are 0%, 2%, 4% and 8% from top to bottom. The spectra were recorded at 303 K. The fractional disorder of the most concentrated sample in each series is indicated. The two mutants show similar disorder at 8% concentration.

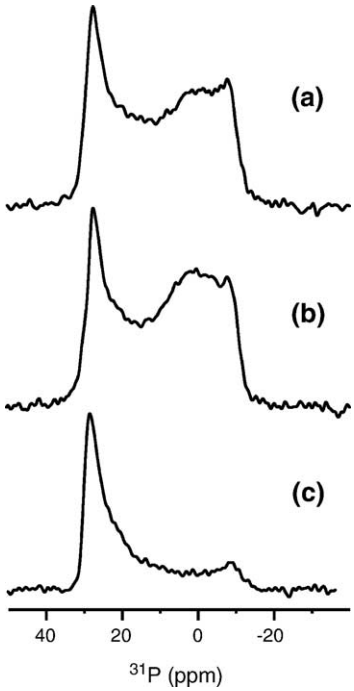

Fig. 4. ^{31}P spectra of oriented *E. coli* lipids in the presence of 4% (a) PG-1, (b) [$\Delta_{4,18}$ G_{10}] PG-1, and (c) [$A_{6,8,13,15}$] PG-1.

abilities seen in model anionic membranes: the deletion mutant causes more severe disorder than the Ala mutant. In fact, the amount of disorder induced by [$\Delta_{4,18}$ G_{10}] PG-1 is comparable to that of wild-type PG-1 (Fig. 4a). Similar to the model membrane results, the type of disorder also differs. [$\Delta_{4,18}$ G_{10}] PG-1 creates significant powder intensities between 15 and −15 ppm and has enhanced intensities at the isotropic frequency, indicative of the onset of an isotropic phase. The Ala mutant merely broadens the 0° peak asymmetrically, indicating a larger mosaic spread of the oriented membrane. The fact that [$\Delta_{4,18}$ G_{10}] PG-1 causes larger disorder to the *E. coli* lipid membrane than to POPE/POPG membranes indicates that stronger electrostatic association facilitates antimicrobial activity since the *E. coli* lipid extracts have a higher anionic charge density than the model membranes used here.

We can gain further insight into the mode of binding of these PG-1 mutants to lipid bilayers by examining the membrane-thickness dependence of the ^{31}P spectra. Fig. 5 shows the spectra of DLPC (12:0), DMPC (14:0) and POPC (16:0,18:1) bilayers containing 4% of the two PG-1 mutants. [$\Delta_{4,18}$ G_{10}] PG-1 shows increasing disorder with the lipid chain length (a–c), whereas [$A_{6,8,13,15}$] PG-1 does not exhibit any dependence on the membrane thickness and only causes minor orientational disorder (d–f). These suggest that [$\Delta_{4,18}$ G_{10}] PG-1, similar to PG-1 [7], has a tendency to insert into the lipid bilayer as long as the hydrophobic length of the peptide and the lipid bilayer are compatible. The wild-type PG-1 has a backbone length of ~30 Å [22]. Combined with the hydrophobic length of the Arg sidechains at the two ends of the molecule, the wild-type PG-1 is able to span the DLPC bilayer without causing orientational defects [7]. This was directly shown by our paramagnetic relaxation study of PG-1 in Mn^{2+}-bound DLPC bilayers [23]. The deletion mutant, which should be shorter than PG-1 by less than ~4 Å, should be able to span the same DLPC bilayer. But compared to the 45 Å thick POPC bilayer, the mismatch is significant enough that the deletion mutant may not be able to insert into the membrane well. Thus, as the bilayer thickness increases, membrane defects form, manifesting themselves as the increased disorder in the ^{31}P spectra.

In contrast, the complete absence of membrane-thickness-dependence of [$A_{6,8,13,15}$] PG-1 suggests that [$A_{6,8,13,15}$] PG-1 binds to the surface of the PC bilayers. The broadened 0° peak in the DMPC spectrum (e) may result from the higher phase transition temperature (23 °C) of this lipid, which may change the slow motion or T_2 relaxation time of the lipid membrane in the presence of the peptide.

3.2. ^{1}H NMR of peptides in solution

The ^{31}P solid-state NMR results above show that the two PG-1 derivatives cause different degrees as well as types of disorder to the lipid bilayers from each other and from the wild-type PG-1. The question then arises as to whether and how the changes in the amino acid sequence and possible changes in peptide conformation bring about this difference in the membrane rupturing abilities. To address this question, we carried out ^{1}H solution NMR experiments on the two mutants and compared their backbone conformation and overall three-dimensional fold with the known structure of PG-1 [24].

Fig. 6 shows the 2D TOCSY spectra of [$\Delta_{4,18}$ G_{10}] PG-1 and [$A_{6,8,13,15}$] PG-1. Significantly different chemical shifts are found, and the deletion mutant exhibits larger shift dispersion than the Ala mutant. Resonance assignment of the amino acid residues was carried out using standard protocols [16]. Sequence-specific assignment was obtained for both peptides due to the presence of sequential connectivities in the 2D NOESY spectra (Fig. 8).

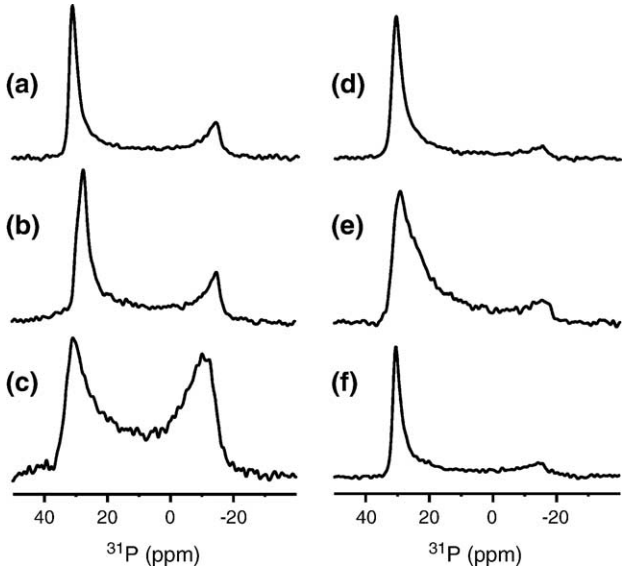

Fig. 5. ^{31}P spectra of oriented phosphocholine bilayers with varying acyl chain lengths in the presence of 4% [$\Delta_{4,18}$ G_{10}] PG-1 (a–c) and 4% [$A_{6,8,13,15}$] PG-1 (d–f). The lipids used are: (a, d) DLPC at 295 K; (b, e) DMPC at 303 K; (c, f) POPC at 295 K.

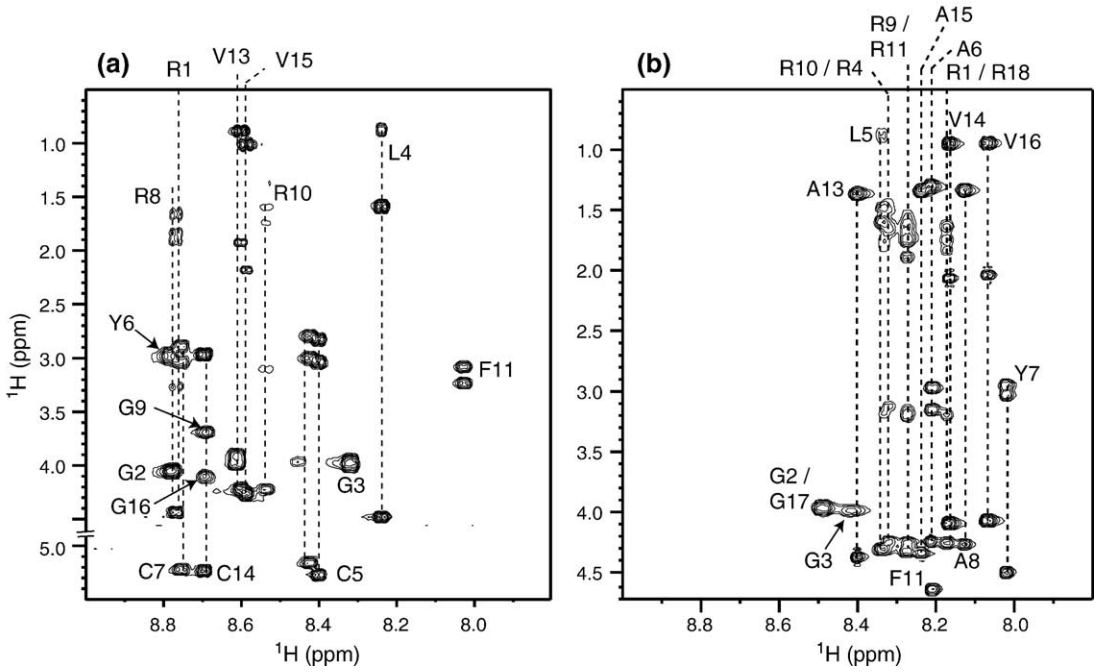

Fig. 6. 2D ^{1}H TOCSY spectra of (a) [$\Delta_{4,18}$ G_{10}] PG-1 and (b) [$A_{6,8,13,15}$] PG-1. Mixing time: 100 ms.

Fig. 7 summarizes the H^N and H^α secondary shifts of the two PG-1 mutants, obtained as the difference of the experimental ^{1}H chemical shifts from the random coil values [25]. For both H^N and H^α, positive secondary shifts indicate a β-sheet conformation while negative secondary shifts indicate an α-helical structure [26]. It can be seen that [$A_{6,8,13,15}$] PG-1 exhibits relatively small secondary shifts, indicating the lack of a well defined secondary structure, while [$\Delta_{4,18}$ G_{10}] PG-1 shows a clear β-sheet conformation.

NOESY spectra allow the determination of the three-dimensional fold of the two mutant peptides. If the hairpin fold is present, then cross-strand correlation peaks are

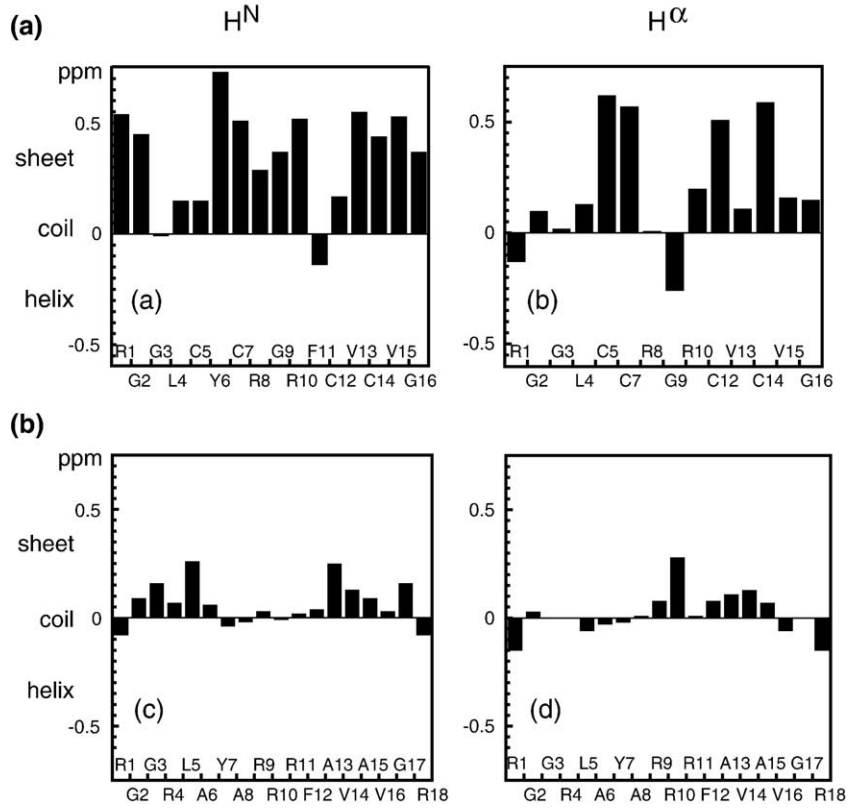

Fig. 7. Differences of H^N and H^α chemical shifts from the random coil values for (a) [$\Delta_{4,18}$ G_{10}] PG-1, and (b) [$A_{6,8,13,15}$] PG-1.

expected. The 2D NOESY spectrum of [$\Delta_{4,18}$ G_{10}] PG-1 shows both sequential αN (i, $i+1$) cross peaks that are characteristic of the β-strand conformation, and cross-strand correlation peaks, including 7/13, 1/15, 3/13 and 6/13 (a). The observed cross-strand connectivities for [$\Delta_{4,18}$ G_{10}] PG-1 are summarized in Fig. 8c. We conclude that [$\Delta_{4,18}$ G_{10}] PG-1 adopts a well-defined β-hairpin fold similar to wild-type PG-1. In contrast, the NOESY spectrum of [$A_{6,8,13,15}$] PG-1 (b) shows no cross-strand correlation peaks but only sequential cross peaks, indicating the lack of a hairpin fold. A COSY experiment on [$A_{6,8,13,15}$] PG-1 indicates that the $^3J_{HN\alpha}$ values of most residues range from 6.8 Hz to 8.3 Hz, whereas the $^3J_{HN\alpha}$ values for the wild-type PG-1 range from 9 Hz to 14 Hz (not shown). These further confirm the lack of a β-strand conformation in [$A_{6,8,13,15}$] PG-1.

4. Discussion

The ^{31}P solid-state NMR and ^1H solution NMR results shown above indicate that the β-hairpin fold is essential for inducing membrane disorder while the reduction in the number of positive charges do not affect the membrane disruptive ability of the peptide significantly. The wild-type PG-1, which possesses both features, inflicts the most severe disorder to anionic membranes [19]. Removing the two disulfide bonds, in [$A_{6,8,13,15}$] PG-1, nearly abolished the membrane-disruptive activity. This is manifested as reduced powder intensities in the ^{31}P spectra of aligned membranes containing [$A_{6,8,13,15}$] PG-1. The main effect of [$A_{6,8,13,15}$] PG-1 appears to be the increase in the mosaic spread of the aligned membrane, broadening the 0° peak (Figs. 2, 3). This is distinct from the lineshape changes observed for other antimicrobial peptides with strong activities such as RTD-1 and PG-1, where significant non 0°-peak intensities are observed and can be attributed to distinct lipid morphologies such as micelles and lipid tubules [8,19]. In comparison, reducing the number of Arg residues from six to three attenuated the membrane disorder but did not remove it. Thus, maintaining the β-hairpin fold is more important than retaining the same number of positive charge as that of the wild-type peptide.

The importance of the β-hairpin fold is consistent with the view that electrostatic association is only the first step in the action of cationic antimicrobial peptides. While the anionic lipopolysaccharides in the outer membrane of Gram-negative bacteria and the anionic DPG and PG lipids in Gram-positive bacteria assist peptide binding, ultimately, membrane disruption requires the bound peptide to adopt the correct conformation to enable it to insert into the membrane.

The requirement for the β-hairpin fold seen in these PG-1 derivatives has also been observed in tachyplesin, a horseshoe-crab derived antimicrobial peptide with similar conformation and charge distribution to PG-1 [27]. A solution NMR study of tachyplesin variants was recently carried out in which Cys residues were systematically replaced by Tyr, Phe or Ala [28]. The study found that the Ala mutant is unstructured in aqueous solution while the Tyr and Phe mutants retain the β-hairpin structure. By varying the solvents, the authors found that the retention of the structure by the Tyr and Phe mutants

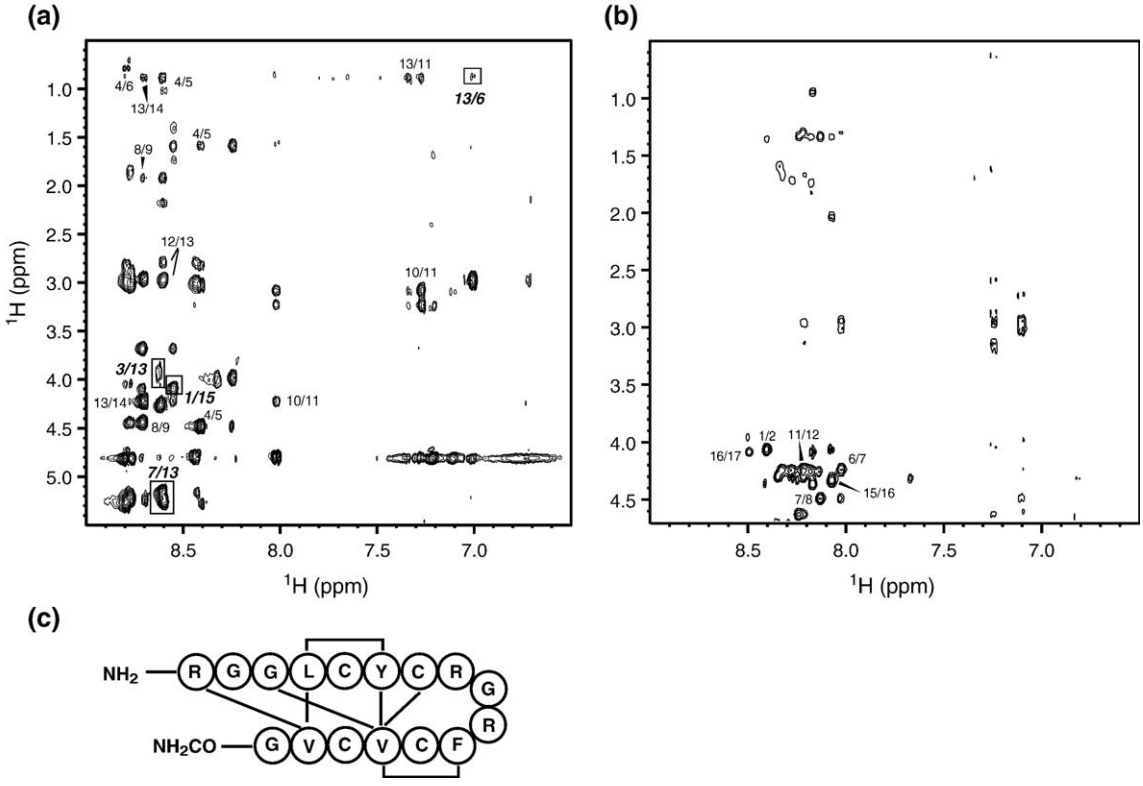

Fig. 8. (a) 2D NOESY spectrum of [$\Delta_{4,18}$ G_{10}] PG-1 with a mixing time of 300 ms. Cross-strand NOE peaks are boxed. (b) 2D NOESY spectrum of [$A_{6,8,13,15}$] PG-1 with a mixing time of 300 ms. (c) Schematic representation of [$\Delta_{4,18}$ G_{10}] PG-1, in which the observed non-sequential NOEs are drawn.

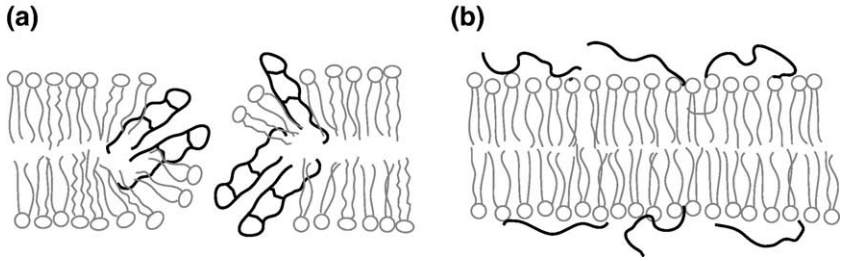

Fig. 9. Models of the different interactions between PG-1 mutants and anionic lipid bilayers. (a) [$\Delta_{4,18}$ G_{10}] PG-1 has a well defined β-hairpin conformation, disrupts the lamellar structure of the lipid membrane, and likely inserts into the bilayer. (b) [$A_{6,8,13,15}$] PG-1 has a random coil conformation in solution, does not cause significant membrane disorder, and likely binds to the surface of the membrane.

is due to aromatic ring stacking interactions. Correspondingly, the Ala mutant has the weakest antimicrobial activity, whereas the Tyr and Phe mutants have strong antimicrobial activities against a number of Gram-positive and Gram-negative bacteria [29].

The ^{1}H solution NMR results of the PG-1 derivatives confirm the design hypothesis that the removal of the disulfide bridges and the lack of any other compensatory interactions result in a random coil peptide in solution [14], whereas the charge-reduced but disulfide-bridged mutant retains its β-strand backbone conformation and the hairpin fold. In SDS micelles and E. Coli mimicking lipids, [$A_{6,8,13,15}$] PG-1 was found to adopt an α-helical conformation by CD [30]. Given the weak activity as well as the weak disorder created by [$A_{6,8,13,15}$] PG-1 to the lipid bilayer, this further underscores the importance of the β-hairpin fold for maintaining the membrane–lytic activity of this class of peptide sequences.

The relative membrane disorder induced by the three PG-1 peptides observed in the ^{31}P spectra correlates well with the measured antimicrobial activities. Normalized to that of PG-1, the minimum inhibitory concentration (MIC) of [$A_{6,8,13,15}$] PG-1 is over 64 fold higher against the Gram-negative bacteria *P. aeruginosa* and more than 16 times higher against the Gram-positive bacteria *Staphylococcus aureus* [14]. The corresponding normalized MIC's for [$\Delta_{4,18}$ G_{10}] PG-1 is >32- and >16-fold that of PG-1. Thus, peptides with stronger antimicrobial activities give rise to larger membrane disorder. The ^{31}P-NMR detected membrane-disruptive ability, the ^{1}H-NMR detected β-hairpin structure, and the antimicrobial activities, all decrease in the order of PG-1> [$\Delta_{4,18}$ G_{10}] PG-1 ≫ [$A_{6,8,13,15}$] PG-1.

The two disulfide-stabilized peptides, PG-1 and [$\Delta_{4,18}$ G_{10}] PG-1, exert less disorder towards POPE/POPG bilayers than towards POPC/POPG bilayers, while the linear analog [$A_{6,8,13,15}$] PG-1 shows no such selectivity. The former suggests that the induction of positive membrane curvature is one mechanism of action of the active protegrins. The only difference between POPC and POPE is that POPE has a smaller headgroup. Thus, POPE can better counter any positive curvature induced by the peptides as they bind to the membrane surface, and thus better maintain the lamellar structure of the bilayer. This positive-curvature mechanism for membrane disruption has also been observed in other peptides such as MSI-78 [10], LL-37 [9] and RTD-1 [8]. The fact that [$A_{6,8,13,15}$] PG-1 does not show such difference is simply a reflection of its generally weaker membrane affinity and disruptive ability.

Fig. 9 gives a schematic representation of our current understanding of the relation between PG-1 mutant conformation and peptide–lipid interaction. The deletion mutant has a β-hairpin structure and efficiently disrupts the membrane structure. It likely achieves this by inserting into the lipid bilayer and creating pores. The Ala mutant, on the other hand, has a random coil conformation in solution and largely retains the membrane integrity. Its lack of membrane-lytic effects may result from a surface-bound location, which is suggested by its lack of dependence on the membrane thickness. The detailed structure of [$\Delta_{4,18}$ G_{10}] PG-1 is not known. For example, how the charged Arg residues are accommodated in the lipid bilayer and the orientation of the hairpin with respect to the lipid chains await further studies. Based on our study of wild-type PG-1, we speculate that [$\Delta_{4,18}$ G_{10}] PG-1 is oligomerized in the membrane [31].

In summary, the results shown here indicate that a correlation indeed exists between the membrane-disruptive ability of a peptide, detected through ^{31}P spectra, and its antimicrobial activity, thus validating the use of ^{31}P NMR of uniaxially aligned membranes for understanding the mechanism of action of antimicrobial peptides. Moreover, the membrane-disruptive ability is related to the conformation of the peptide: for protegrins, a strong β-hairpin fold is correlated with potent membrane disruption. Between the two structural features examined, charge and β-sheet conformation, the number of charges is a secondary factor that regulates the strength of the interaction between the anionic membrane and the cationic peptide. The more important structure requirement for antimicrobial activity in this class of peptide sequences is the β-hairpin fold. As investigated previously through extensive sequence mutations [27,32], the importance of the β-hairpin fold may result from the fact that it places the hydrophobic and charged residues in these peptides in an amphipathic fashion, in order to promote the insertion of the peptides into the lipid bilayers.

Acknowledgements

The authors thank Dr. Bruce Fulton for expert help with the solution NMR experiments and Prof. Amy Andreotti for helpful discussions.

This work is supported by the National Institutes of Health grant GM-066976 to M. Hong and grants AI-22839 and AI-37945 to A.J. Waring and R.I. Lehrer.

References

[1] E. Strandberg, A.S. Ulrich, NMR methods for studying membrane-active antimicrobial peptides, Concepts Magn. Reson. 23 (2004) 89–120.
[2] B. Bechinger, The structure, dynamics, and orientation of antimicrobial peptides in membranes by multidimensional solid-state NMR spectroscopy, Biochim. Biophys. Acta 1462 (1999) 157–183.
[3] I.C.P. Smith, I.H. Ekiel, in: I.C. Gorenstein (Ed.), Phosphorous-31 NMR: Principles and Applications, Academic Press, Inc., 1984, pp. 447–475.
[4] E.J. Prenner, R.N.L. RN, K.C. Neuman, S.M. Gruner, L.H. Kondejewski, R.S. Hodges, R.N. McElhaney, Nonlamellar phases induced by the interaction of gramicidin S with lipid bilayers. A possible relationship to membrane-disrupting activity, Biochemistry 36 (1997) 7906–7916.
[5] B.B. Bonev, R.J. Gilbert, P.W. Andrew, O. Byron, A. Watts, Structural analysis of the protein/lipid complexes associated with pore formation by the bacterial toxin pneumolysin, J. Biol. Chem. 276 (2001) 5714–5719.
[6] G. Anderluh, M.D. Serra, G. Viero, G. Guella, P. Macek, G. Menestrina, Pore formation by equinatoxin II, a eukaryotic protein toxin, occurs by induction of nonlamellar lipid structures, J. Biol. Chem. 278 (2003) 45216–45223.
[7] S. Yamaguchi, T. Hong, A. Waring, R.I. Lehrer, M. Hong, Solid-state NMR investigations of peptide–lipid interaction and orientation of a beta-sheet antimicrobial peptide, protegrin, Biochemistry 41 (2002) 9852–9862.
[8] J.J. Buffy, M.J. McCormick, S. Wi, A. Waring, R.I. Lehrer, M. Hong, Solid-State NMR investigation of the selective perturbation of lipid bilayers by the cyclic antimicrobial peptide RTD-1, Biochemistry 43 (2004) 9800–9812.
[9] K.A. Henzler Wildman, D.K. Lee, A. Ramamoorthy, Mechanism of lipid bilayer disruption by the human antimicrobial peptide, LL-37, Biochemistry 42 (2003) 6545–6558.
[10] K.J. Hallock, D.K. Lee, A. Ramamoorthy, MSI-78, an analogue of the magainin antimicrobial peptides, disrupts lipid bilayer structure via positive curvature strain, Biophys. J. 84 (2003) 3052–3060.
[11] M.S. Balla, J.H. Bowie, F. Separovic, Solid-state NMR study of antimicrobial peptides from Australian frogs in phospholipid membranes, Eur. Biophys. J. 33 (2004) 109–116.
[12] V.N. Kokryakov, S.S. Harwig, E.A. Panyutich, A.A. Shevchenko, G.M. Aleshina, O.V. Shamova, H.A. Korneva, R.I. Lehrer, Protegrins: leukocyte antimicrobial peptides that combine features of corticostatic defensins and tachyplesins, FEBS Lett. 327 (1993) 231–236.
[13] L. Bellm, R.I. Lehrer, T. Ganz, Protegrins: new antibiotics of mammalian origin, Exp. Opin. Invest. Drugs 9 (2000) 1731–1742.
[14] J. Chen, T.J. Falla, H. Liu, M.A. Hurst, C.A. Fujii, D.A. Mosca, J.R. Embree, D.J. Loury, P.A. Radel, C. Cheng Chang, L. Gu, J.C. Fiddes, Development of protegrins for the treatment and prevention of oral mucositis: structure–activity relationships of synthetic protegrin analogues, Biopolymers 55 (2000) 88–98.
[15] K.J. Hallock, K. Henzler Wildman, D.K. Lee, A. Ramamoorthy, An innovative procedure using a sublimable solid to align lipid bilayers for solid-state NMR studies, Biophys. J. 82 (2002) 2499–2503.
[16] K. Wuthrich, NMR of Proteins and Nucleic Acids, John Wiley, New York, 1986.
[17] M. Piotto, V. Saudek, V. Sklenar, Gradient-tailored excitation for single-quantum NMR spectroscopy of aqueous solutions, J. Biomol. NMR 2 (1992) 661–665.
[18] A.J. Shaka, C.J. Lee, A. Pines, Iterative schemes for bilinear operators—Application to spin decoupling, J. Magn. Reson. 77 (1988) 274–293.
[19] R. Mani, J.J. Buffy, A.J. Waring, R.I. Lehrer, M. Hong, Solid-state NMR investigation of the selective disruption of lipid membranes by protegrin-1, Biochemistry 43 (2004) 13839–13848.
[20] C. Ratledge, S.G. Wilkinson, Microbial Lipids, vol. 1, Academic Press, London, 1988.
[21] L.K. Nicholson, F. Moll, T.E. Mixon, P.V. LoGrasso, J.C. Lay, T.A. Cross, Solid-state 15N NMR of oriented lipid bilayer bound gramicidin A, Biochemistry 26 (1987) 6621–6626.
[22] D.H. Jones, S.J. Opella, Weak alignment of membrane proteins in stressed polyacrylamide gels, J. Magn. Reson. 171 (2004) 258–269.
[23] J.J. Buffy, T. Hong, S. Yamaguchi, A. Waring, R.I. Lehrer, M. Hong, Solid-state NMR investigation of the depth of insertion of protegin-1 in lipid bilayers using paramagnetic Mn2+, Biophys. J. 85 (2003) 2363–2373.
[24] R.L. Fahrner, T. Dieckmann, S.S. Harwig, R.I. Lehrer, D. Eisenberg, J. Feigon, Solution structure of protegrin-1, a broad-spectrum antimicrobial peptide from porcine leukocytes, Chem. Biol. 3 (1996) 543–550.
[25] H. Zhang, S. Neal, D.S. Wishart, RefDB: a database of uniformly referenced protein chemical shifts, J. Biomol. NMR 25 (2003) 173–195.
[26] D.S. Wishart, B.D. Sykes, F.M. Richards, Relationship between nuclear magnetic resonance chemical shift and protein secondary structure, J. Mol. Biol. 222 (1991) 311–333.
[27] S.A. Muhle, J.P. Tam, Design of Gram-negative selective antimicrobial peptides, Biochemistry 40 (2001) 5777–5785.
[28] A. Laederach, A.H. Andreotti, D.B. Fulton, Solution and micelle-bound structures of tachyplesin I and its active aromatic linear derivatives, Biochemistry 41 (2002) 12359–12368.
[29] A.G. Rao, Conformation and antimicrobial activity of linear derivatives of tachyplesin lacking disulfide bonds, Arch. Biochem. Biophys. 361 (1999) 127–134.
[30] S.S. Harwig, A. Waring, H.J. Yang, Y. Cho, L. Tan, R.I. Lehrer, Intramolecular disulfide bonds enhance the antimicrobial and lytic activities of protegrins at physiological sodium chloride concentrations, Eur. J. Biochem. 240 (1996) 352–357.
[31] J.J. Buffy, A.J. Waring, M. Hong, Determination of peptide oligomerization in lipid membranes with magic-angle spinning spin diffusion NMR, J. Am. Chem. Soc. 127 (2005) 4477–4483.
[32] J.P. Tam, C. Wu, J.L. Yang, Membranolytic selectivity of cystine-stabilized cyclic protegrins, Eur. J. Biochem. 267 (2000) 3289–3300.